

## Supporting Information

# The Semi-Closed Molten Salt-Assisted One-Step Synthesis of N-P-Fe Tridoped Porous Carbon Nanotubes for an Efficient Oxygen Reduction Reaction

Jianghai Deng <sup>1,\*</sup> and Qiuyun Zhou <sup>2</sup>

<sup>1</sup> Nuclear Power Institute of China, Chengdu 610000, China

<sup>2</sup> Chongqing Changan New Energy Vehicles Technology Co., Ltd.,  
Chongqing 401120, China

\* Correspondence: scudeng@163.com

## 1. Characterization

The structure and morphology of the samples were characterized by scanning electron microscopy (SEM) and transmission electron microscopy (TEM, Zeiss LIBRA 200 FETEM, 200 kV). Powder X-ray diffraction data were obtained from an XRD-6000 using Cu KR radiation at a step rate of 5° min<sup>-1</sup>. X-ray Photoelectron Spectroscopy (XPS) analysis was performed on a PE PHI-5400 spectrometer equipped with a monochromatic Al X-ray source (Al KR, 1.4866 KeV). The degree of graphitization was tested by Raman spectroscopy techniques (Lab Ram HR evolution, excited by a 532 nm laser).

## 2. Electrochemical Measurements

**RDE test:** The electrochemical experiments were carried out on a standard three-electrode cell at room temperature. A glassy carbon was used as a working electrode (GC electrode, 5 mm in diameter, PINE: AFE3T050GC), Ag/AgCl (saturated KCl) as a reference electrode, and carbon rod as the counter electrode. The working electrodes were prepared by applying catalyst ink onto glassy carbon (GC) disk electrodes. The loading of the catalyst is 0.5 mg cm<sup>-2</sup> and the commercial Pt/C is 25 ug<sub>Pt</sub> cm<sup>-2</sup>. The activities of catalysts were evaluated by linear sweep voltammetry (LSV) curves obtained in the O<sub>2</sub>-saturated 0.1 M KOH solution at a potential scan rate of 10 mVs<sup>-1</sup> and a rotation speed of 1600 rpm.

The electron transfer number (n) was acquired by Koutecky-Levich equations.

$$\frac{1}{J} = \frac{1}{J_D} + \frac{1}{J_K} = \frac{1}{B\omega^{1/2}} + \frac{1}{J_K} \quad (S1)$$

$$B = 0.62nFC_0(D_0)^{2/3}\nu^{-1/6} \quad (S2)$$

In the equations  $J$  ;  $J_K$  and  $J_D$  are the measured current density, the kinetic and diffusion-limiting current densities respectively.  $\omega$  is the angular velocity of the disk.  $n$  is the overall electrons transfer number in ORR,  $F$  is the Faraday constant ( $F = 96,485 \text{ C mol}^{-1}$ ),  $C_0$  is the bulk concentration of  $O_2$ ,  $\nu$  is the kinematic viscosity of the electrolyte, and  $k$  is the electron transfer rate constant. In 0.1 MKOH the  $C_0 = 1.2 \times 10^{-3} \text{ mol L}^{-1}$ ,  $D_0 = 1.9 \times 10^{-5} \text{ cm}^2 \text{ s}^{-1}$  and  $\nu = 0.1 \text{ m}^2 \text{ s}^{-1}$ .

The accelerated durability test (ADT) was carried out by CV test at potentials between 0.6 and 1.1 V vs RHE and a scan rate of  $50 \text{ mVs}^{-1}$  in oxygen-saturated 0.1 M KOH at room temperature.

**Zn-O<sub>2</sub> battery :** The Zinc-Air battery test was carried out using a home-made Zn-O<sub>2</sub> battery in a 6 M KOH solution, and pure oxygen was used as cathode reactant. Both the loading of P-FeNC/CNT and commercial Pt/C (20%) are  $0.5 \text{ mg cm}^{-2}$ . The catalysts ink was prepared by dispersing 2 mg catalysts in 195  $\mu\text{L}$  alcohol and 5  $\mu\text{L}$  nafion (5 wt.%) solution. Then the catalysts ink was uniformly coated onto the carbon paper and dried at room temperature. A Zn plate and the carbon paper with catalysts were used as the anode and cathode respectively. A piece of nickel foam was used as the current collector. Both electrodes and the current collector were assembled into the Zn-O<sub>2</sub> battery. The polarization curves were recorded by linear sweep voltammetry (LSV) at a sweep rate of  $10 \text{ mV s}^{-1}$ .

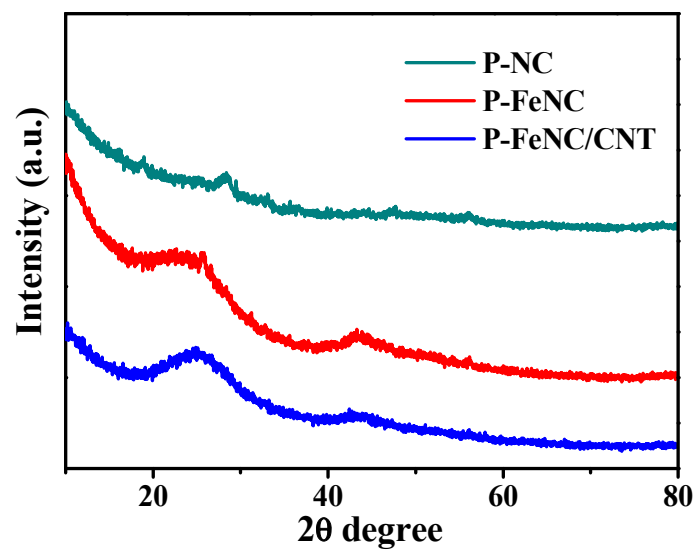


**Figure S1.** XRD patterns of P-NC, P-FeNC and P-FeNC/CNT.

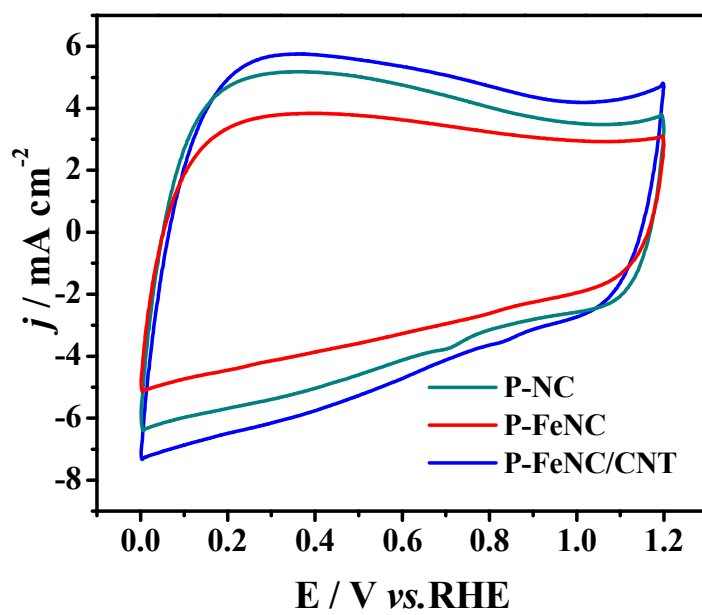


**Figure S2.** CV curves of the as prepared catalysts in O<sub>2</sub>-saturated 0.1M KOH at a sweep rate of 50 mVs<sup>-1</sup>.

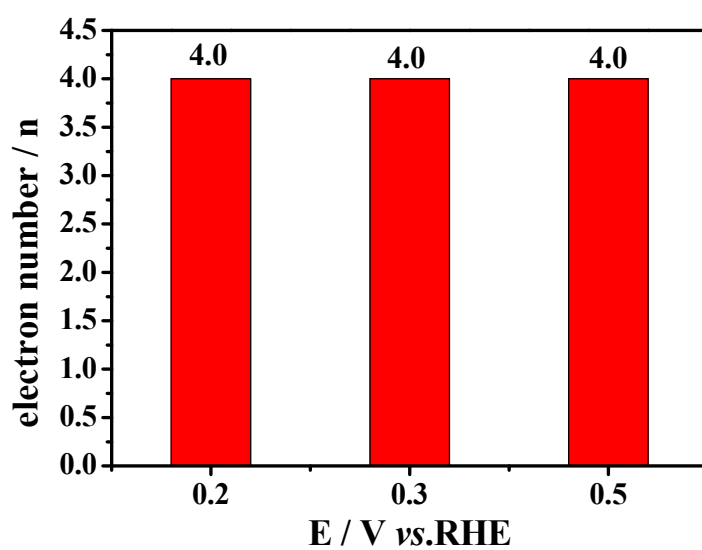


Figure S3. The electron transfer numbers (n) of P-FeNC/CNT.

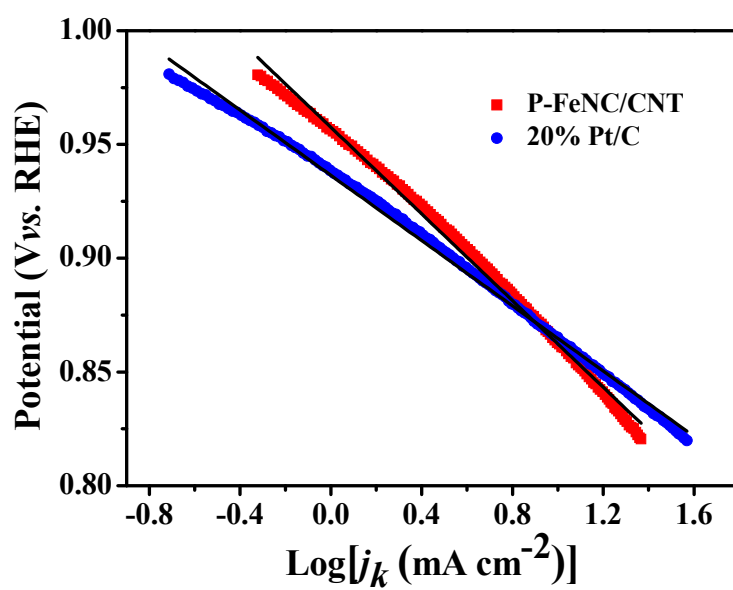
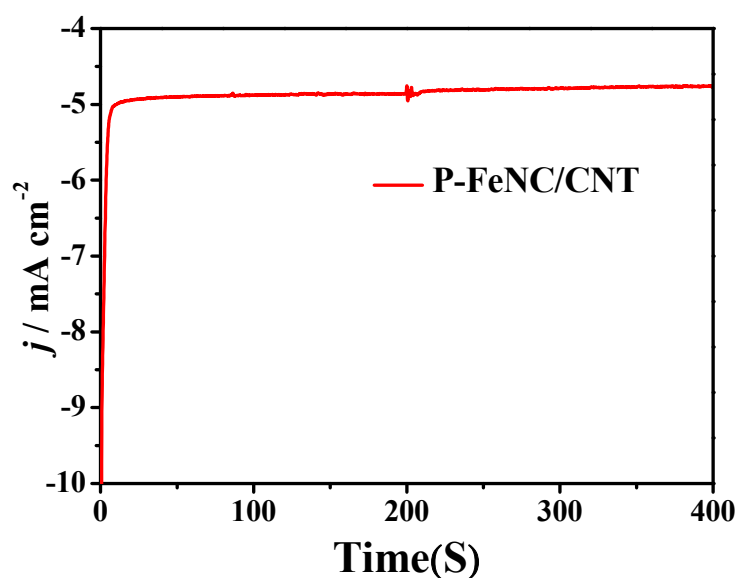
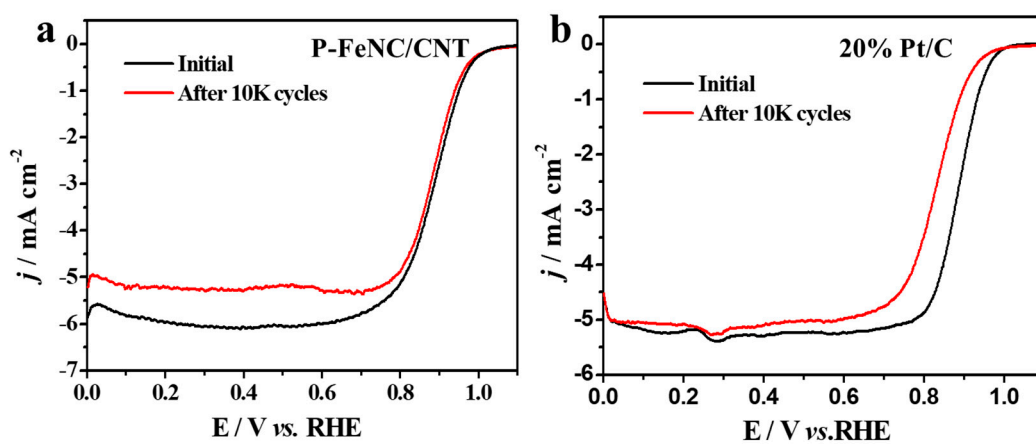


Figure S4. Tafel slopes of P-FeNC/CNT and Pt/C.



**Figure S5.** Current-time curve of P-FeNC/CNT catalysts in O<sub>2</sub>-saturated 0.1 M KOH, before and after the addition of 0.5 M CH<sub>3</sub>OH.



**Figure S6.** Polarization curves of the P-FeNC/CNT and commercial Pt/C catalysts in O<sub>2</sub>-saturated 0.1M KOH at 1600 rpm with a sweep rate of 10 mV s<sup>-1</sup> before and after the accelerated durability test. (a) P-Fe-NC catalyst. (b) Commercial Pt/C.

**Table S1.** The element content of P-FeNC/CNT catalyst obtained from XPS and the Fe content obtained form ICP-MS.

Sample	C(at.%)	N(at.%)	O(at.%)	P(at.%)	Fe(at.%)	ICP-MS Fe(wt%)
P-FeNC/CNT	88.26	1.88	7.8	1.76	0.3	1.31

**Table S2.** Comparison of the ORR activity of P-FeNC/CNT catalyst with other reported electrocatalysts in alkaline electrolytes with a rotation rate of 1600 rpm.

catalysts	Dopant atoms	Loading (mg cm <sup>-2</sup> )	Half-wave Potential (V)	References
<b>P-FeNC/CNT</b>	<b>Fe;N;P</b>	<b>0.5</b>	<b>0.89</b>	<b>This work</b>
Co-P,N-CNT	Co;N;P	--	0.827	S1
Fe2P(3 nm)@BC	Fe;N;P;S	0.425	0.82	S2
Fe-NBC-2	Fe;N;B	0.2	0.86	S3
3D MPC	Fe;N	0.5	0.88	S4
Fe-NMCSs	Fe;N	0.255	0.86	S5
NB-CN	Co;N;B	--	0.835	S6
Fe-NPC	Fe;P;N	0.5	0.885	S7
pCNT@Fe@GL	Fe;N	--	0.87	S8
FeCo-Nx-CN-30	Fe;Co;N	0.1	0.886	S9
N0.54-Z3/M1-900	N;C	0.25	0.824	S10
NPMC-1000	N,P	0.15	0.85	S11

**Table S3.** Comparison of the power density of Zn-O<sub>2</sub> batteries in this work with other reported electrocatalysts.

Catalysts	Electrolyte	Cathod	Power Density mW cm <sup>-2</sup>	References
Pt/C	6 M KOH	O <sub>2</sub>	190	This work
P-FeNC/CNT	6 M KOH	O <sub>2</sub>	240	This work
Fe/N/C-ZnCl <sub>2</sub> /KCl	6 M KOH	O <sub>2</sub>	206	S12
NPMC	6 M KOH + 0.2 M Zn(Ac) <sub>2</sub>	Air	55	S11
NiFeP	6 M KOH + 0.2 M Zn(Ac) <sub>2</sub>	O <sub>2</sub>	220	S13
Fe/N/C	6 M KOH	O <sub>2</sub>	235	S14
FeCo-Nx	6 M KOH + 0.2 M Zn(Ac) <sub>2</sub>	Air	150	S9
NCNT/CoO	6 M KOH + 0.2 M Zn(Ac) <sub>2</sub>	Air	102	S15
Ag-Cu	6 M KOH + 0.2 M Zn(Ac) <sub>2</sub>	Air	67	S16
Co(OH) <sub>2</sub> +N	6 M KOH	Air	36	S17
Co <sub>3</sub> O <sub>4</sub> NW	6 M KOH	Air	40	S18
C-CoPAN	6 M KOH + 0.2 M Zn(Ac) <sub>2</sub>	Air	125	S19



## References in Supporting Information

- S1. Guo, S.; Yuan, P.; Zhang, J.; Jin, P.; Sun, H.; Lei, K.; Pang, X.; Xu, Q.; Cheng, F. Atomic-scaled cobalt encapsulated in P,N-doped carbon sheaths over carbon nanotubes for enhanced oxygen reduction electrocatalysis under acidic and alkaline media. *Chem. Commun.* **2017**, 53, 9862–9865.
- S2. Ye, Y.; Duan, W.; Yi, X.; Lei, Z.; Li, G.; Feng, C. Biogenic precursor to size-controlled synthesis of Fe<sub>2</sub>P nanoparticles in heteroatom-doped graphene-like carbons and their electrocatalytic reduction of oxygen. *J. Power Sources* **2019**, 435, 226770.
- S3. Li, Y.; Li, Z.; Wu, Y.; Wu, H.; Zhang, H.; Wu, T.; Yuan, C.; Xu, Y.; Zeng, B.; Dai, L. Carbon particles co-doped with N, B and Fe from metal-organic supramolecular polymers for boosted oxygen reduction performance. *J. Power Sources* **2019**, 412, 623–630.
- S4. Wang, W.; Chen, W.; Miao, P.; Luo, J.; Wei, Z.; Chen, S. NaCl Crystallites as Dual-Functional and Water-Removable Templates To Synthesize a Three-Dimensional Graphene-like Macroporous Fe-N-C Catalyst. *ACS Catal.* **2017**, 7, 6144–6149.
- S5. Meng, F.-L.; Wang, Z.-L.; Zhong, H.-X.; Wang, J.; Yan, J.-M.; Zhang, X.-B. Reactive Multifunctional Template-Induced Preparation of Fe-N-Doped Mesoporous Carbon Microspheres Towards Highly Efficient Electrocatalysts for Oxygen Reduction. *Adv. Mater.* **2016**, 28, 7948–7955.
- S6. Lu, Z.; Wang, J.; Huang, S.; Hou, Y.; Li, Y.; Zhao, Y.; Mu, S.; Zhang, J.; Zhao, Y. N,B-codoped defect-rich graphitic carbon nanocages as high performance multifunctional electrocatalysts. *Nano Energy* **2017**, 42, 334–340.
- S7. Li, Y.; Chen, B.; Duan, X.; Chen, S.; Liu, D.; Zang, K.; Si, R.; Lou, F.; Wang, X.; Rønning, M.; et al. Atomically dispersed Fe-N-P-C complex electrocatalysts for superior oxygen reduction. *Appl. Catal. B Environ.* **2019**, 249, 306–315.
- S8. Ahn, S.H.; Yu, X.; Manthiram, A. “Wiring” Fe-N<sub>x</sub>-Embedded Porous Carbon Framework onto 1D Nanotubes for Efficient Oxygen Reduction Reaction in Alkaline and Acidic Media. *Adv. Mater.* **2017**, 29, 1606534.
- S9. Li, S.; Cheng, C.; Zhao, X.; Schmidt, J.; Thomas, A. Active Salt/Silica-Templated 2D Mesoporous FeCo-N<sub>x</sub>-Carbon as Bifunctional Oxygen Electrodes for Zinc–Air Batteries. *Angew. Chem. Int. Ed.* **2018**, 57, 1856–1862.
- S10. Li, X.G.; Guan, B.Y.; Gao, S.Y.; Lou, X. A general dual-templating approach to biomass-derived hierarchically porous heteroatom-doped carbon materials for enhanced electrocatalytic oxygen reduction. *Energy Environ. Sci.* **2019**, 12, 648–655.
- S11. Zhang, J.; Zhao, Z.; Xia, Z.; Dai, L. A metal-free bifunctional electrocatalyst for oxygen reduction and oxygen evolution reactions. *Nat. Nanotechnol.* **2015**, 10, 444–452.
- S12. Li, J.; Chen, S.; Li, W.; Wu, R.; Ibraheem, S.; Li, J.; Ding, W.; Li, L.; Wei, Z. A eutectic salt-assisted semi-closed pyrolysis route to fabricate high-density active-site hierarchically porous Fe/N/C catalysts for the oxygen reduction reaction. *J. Mater. Chem. A* **2018**, 6, 15504–15509.
- S13. Ibraheem, S.; Chen, S.; Li, J.; Li, W.; Gao, X.; Wang, Q.; Wei, Z. Three-Dimensional Fe,N-Decorated Carbon-Supported NiFeP Nanoparticles as an Efficient Bifunctional Catalyst for Rechargeable Zinc–O<sub>2</sub> Batteries. *ACS Appl. Mater. Interfaces* **2018**, 11, 699–705.
- S14. Wang, M.; Qian, T.; Zhou, J.; Yan, C. An efficient bifunctional electrocatalyst for a zinc–air battery derived from Fe/N/C and bimetallic metal–organic framework composites. *ACS Appl. Mater. Interfaces* **2017**, 9, 5213–5221.
- S15. Liu, X.; Park, M.; Kim, M.G.; Gupta, S.; Wu, G.; Cho, J. Integrating NiCo Alloys with Their Oxides as Efficient Bifunctional Cathode Catalysts for Rechargeable Zinc–Air Batteries. *Angew. Chem. Int. Ed.* **2015**, 54, 9654–9658.
- S16. Lei, Y.; Chen, F.; Jin, Y.; Liu, Z. Ag-Cu nanoalloyed film as a high-performance cathode electrocatalytic material for zinc-air battery. *Nanoscale Res. Lett.* **2015**, 10, 197.
- S17. Sharifi, T.; Espino, E.G.; Jia, X.; Sandström, R.; Wågberg, T. Comprehensive study of an earth-abundant bifunctional 3D electrode for efficient water electrolysis in alkaline medium. *ACS Appl. Mater. Interfaces* **2015**, 7, 28148–28155.

- S18. Lee, D.U.; Choi, J.Y.; Feng, K.; Park, H.W.; Chen, Z. Advanced extremely durable 3D bifunctional air electrodes for rechargeable zinc - air batteries. *Adv. Energy Materials* **2014**, 4, 1301389.
- S19. Li, B.; Ge, X.; Goh, F.W.T.; Hor, T.S.A.; Geng, D.; Du, G.; Liu, Z.; Zhang, J.; Liu, X.; Zong, Y. Co<sub>3</sub>O<sub>4</sub> nanoparticles decorated carbon nanofiber mat as binder-free air-cathode for high performance rechargeable zinc-air batteries. *Nanoscale* **2015**, 7, 1830–1838.